

## Combination of $D^{*\pm}$ Differential Cross-Section Measurements in Deep-Inelastic ep Scattering at HERA

Jan Hladky<sup>1\*</sup>

*Institute of Physics, Acad. Sci. Czech Rep.*

*182 21 Prague 8, Na Slovance 2, Czech Republic*

*E-mail: [hladky@fzu.cz](mailto:hladky@fzu.cz)*

H1 and ZEUS have published single differential cross sections for inclusive  $D^{*\pm}$ -meson production in deep-inelastic *electron-proton* scattering at HERA from their respective final data sets. The cross sections are here combined in common visible phase space region of photon virtuality  $Q^2 > 5 \text{ GeV}^2$ , electron inelasticity  $0.02 < y < 0.7$  and  $D^{*\pm}$  meson's transverse momentum  $p_T(D^{*\pm}) > 1.5 \text{ GeV}$  and pseudorapidity  $|\eta(D^{*\pm})| < 1.5$ . The combination procedure takes into account all correlations, yielding significantly reduced experimental uncertainties. Double differential cross-sections  $d^2\sigma/dQ^2dy$  are combined with earlier  $D^{*\pm}$  data, extending the kinematic range down to  $Q^2 > 1.5 \text{ GeV}^2$ . Perturbative next-to-leading-order QCD predictions are compared with the experimental results obtained.

*The European Physical Society Conference on High Energy Physics  
22–29 July 2015  
Vienna, Austria*

---

<sup>1</sup>Speaker

\*On behalf of [H1](#) and [ZEUS](#) Collaborations [DESY in Hamburg](#)

## 1. Introduction

DESY in Hamburg produced data up to year 2007 using *electron-proton* collider HERA. Experiments *H1* and *ZEUS* have studied there in *Deep-Inelastic-Scattering* (*DIS*) single and double differential cross-sections  $d\sigma$  of inclusive  $D^{*\pm}$  meson production and have their respective results published in the past time [1]. In recent time new combination of both data are made and presented here. Study of open *charm* production in *DIS* at HERA provides important input for stringent tests of the strong interaction theory – quantum chromodynamics (QCD). Previous measurements of charm production in *DIS* at HERA have shown that *charm* quarks are predominantly produced in boson-gluon fusion process. *Charm* production becomes sensitive to gluon distribution in the proton. There is also sensitivity to *c* and *b* quark masses.

Measurements have been made in DESY and the data from *HERA-I* and *HERA-II* are obtained. The full reconstruction of *charm* mesons  $D^0$  and  $D^{*\pm}$  produced in *DIS* is reached. Two different methods can be used to extract the cross-sections. Here, alternatively to previous studies, the measured cross sections in both experiments can be combined directly in the visible phase space. The method used minimal extrapolation and is fewer dependent on theory assumptions. But the data used should have the same final state, covering a common visible phase space. The visible  $D^{*\pm}$  meson production cross sections at center of mass energy  $s^{1/2} = 318$  GeV are combined such that one consistent *HERA* data set is obtained and compared directly to the differential next-to-leading-order (NLO) QCD predictions. The procedure used yields a significant reductions of overall uncertainties of the measurements.

## 2. Theoretical predictions

FFNS (Fixed-Flavour-Number-Scheme) – 3 flavour is used for theoretical predictions [2]. Available are NLO calculations. HVQDIS [3] program provided NLO QCD ( $O(\alpha_s^2)$ ) calculations for  $d\sigma$  predictions of  $D^{*\pm}$  meson production have been used.

Parameters used for prediction's uncertainties estimation:

\* renormalisation and factorisation scale  $\mu_r = \mu_f = (Q^2 + 4m_c^2)^{1/2}$

\* pole mass of *charm* quark  $m_c = 1.50 \pm 0.15$  GeV

\* strong coupling constant  $\alpha_s^{n_f=3}(M_Z) = 0.105 \pm 0.002$

\* proton PDFs are described as used in HERAFitter [4]

\* fraction  $f$  of charm quarks hadronising to  $D^{*\pm}$  is  $0.2287 \pm 0.0056$

\* fragmentation parameter  $\alpha_K$ , bin boundary  $s_I$ ,  $\langle k_T \rangle$  - as usually varied.

For **beauty** quarks are parameters for predictions uncertainties estimation also calculated. Contribution of **beauty** hadrons to  $D^{*\pm}$  signal is small.

### 3. Data samples for cross-section combinations

The **H1** and **ZEUS** detectors - see **Fig. 1**. Central tracker detectors (*CTD*) operated inside solenoidal magnetic fields of 1.16 T (**H1**) and 1.43 T (**ZEUS**). Electromagnetic sections of the calorimeters measured charged particles trajectories in polar angular range of  $15 < \Theta^\circ < 165$  or (164). For charged particles passing all Si vertex detectors and *CTDs* is transverse momentum resolutions of  $\sigma(p_T)/p_T \sim 0.002p_T + 0.015$  (**H1**) and  $\sim 0.0029p_T + 0.0081 + 0.0012/p_T$  (**ZEUS**) - ( $p_T$  in GeV). Resolution of scattered  $e^\pm$  electromagnetic energy  $E$  is:  $\sigma(E)/E$  of  $0.11/E^{1/2}$  in LAr and  $0.07/E^{1/2}$  in SpaCal (**H1**) and of  $0.18/E^{1/2}$  (**ZEUS**) - ( $E$  in GeV).

Luminosity is known with a precision of 3.2% (**H1**) and  $\sim 2\%$  (**ZEUS**).

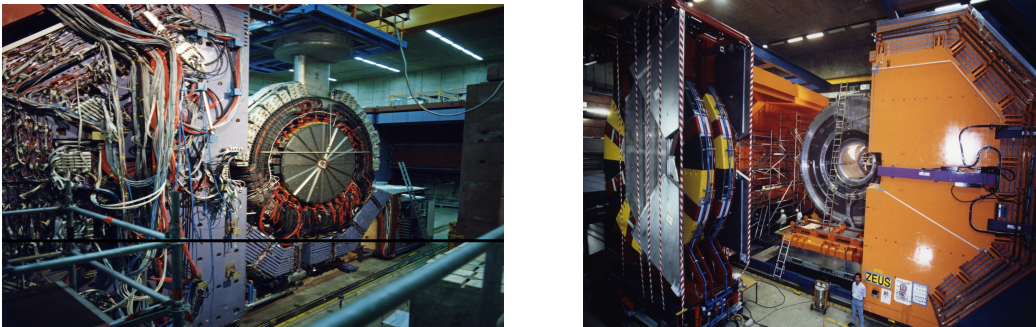


**Fig. 1.** The detectors. **H1** - left in blue and **ZEUS** - right in orange colours.

Data sets used for combinations of both experiments, their kinematic range and luminosity are presented in the Table 1. Typical  $D^{*\pm}$  meson signal is seen in **Fig. 2**.

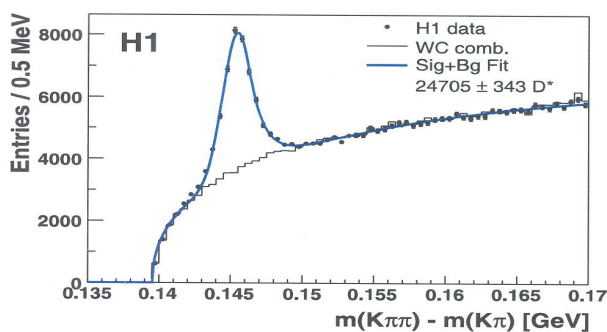


**Fig. 2.** Typical  $D^{*\pm}$  meson signal.

Data set				Kinematic range				$\mathcal{L}$ (pb <sup>-1</sup> )
				$Q^2$ (GeV <sup>2</sup> )	$y$	$p_T(D^*)$ (GeV)	$\eta(D^*)$	
I	H1 $D^{*\pm}$ HERA-II (medium $Q^2$ )	[18]	5 : 100	0.02 : 0.70	> 1.5	-1.5 : 1.5	348	
II	H1 $D^{*\pm}$ HERA-II (high $Q^2$ )	[15]	100 : 1000	0.02 : 0.70	> 1.5	-1.5 : 1.5	351	
III	ZEUS $D^{*\pm}$ HERA-II	[20]	5 : 1000	0.02 : 0.70	1.5 : 20.0	-1.5 : 1.5	363	
IV	ZEUS $D^{*\pm}$ 98-00	[6]	1.5 : 1000	0.02 : 0.70	1.5 : 15.0	-1.5 : 1.5	82	

Table 1: Data sets used in the combination. For each data set the respective kinematic range and the integrated luminosity,  $\mathcal{L}$ , are given.

Two types of the data combinations are performed - for: a/ single-differential cross section  $d\sigma$  and b/ double-differential cross section  $d^2\sigma$ .

a/ - data sets I ÷ III (see Table 1) have been used and the combinations for the  $d\sigma(D^{*\pm})$  vs. transverse momentum  $p_T(D^{*\pm})$ , pseudorapidity  $\eta(D^{*\pm})$  and inelasticity  $z(D^{*\pm})$  made - see e.g. for  $p_T(D^{*\pm})$  on **Fig. 3**

b/ - all four data sets can be used for the combinations and reconstruction of the  $d^2\sigma/dQ^2 dy(D^{*\pm})$  - see **Fig. 6**.

#### 4. Combination method

The following actions for the data combination procedures have been performed:

- \* the data sets combination uses the  $\chi^2$  minimisation method in program HERAverager
- \* correlated and uncorrelated systematic uncertainties fully taken into account - (are predominantly of multiplicative nature)
- \* statistical uncertainties are mostly background dominated
- \* almost all experimental systematic uncertainties are treated as independent between **H1** and **ZEUS** data sets (since the distributions of  $p_T(D^{*\pm})$ ,  $\eta(D^{*\pm})$ ,  $z(D^{*\pm})$ ,  $Q^2$  and  $y$  are not statistically independent, each distribution is combined separately)
- \* for the single-differential cross section  $d\sigma$  combinations reach theory uncertainties 0 ÷ 10% of total
- \* several double-differential cross section  $d^2\sigma$  intervals were combined using the shape HVQDIS predictions program.

## 5. Combined cross sections

As one can see, datasets for combinations of single-differential cross section  $d\sigma(D^{*\pm})$  vs.  $p_T(D^{*\pm})$ ,  $z(D^{*\pm})$  and also other values mentioned above (from only HERA II data) performed and presented - see e.g. in **Fig. 3**. for the  $d\sigma(D^{*\pm})$  vs.  $p_T(D^{*\pm})$ , are consistent. The inner error bars indicate the uncorrelated part of the uncertainties, the outer error bars the total uncertainties. The histogram indicate the binning used to calculate the cross sections. Its bottom part shows the ratio of the cross sections with respect to the central value of the combined cross sections.

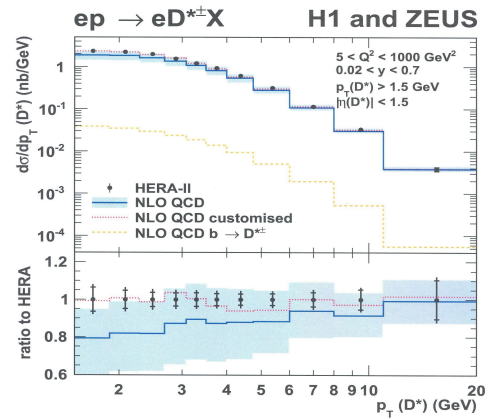
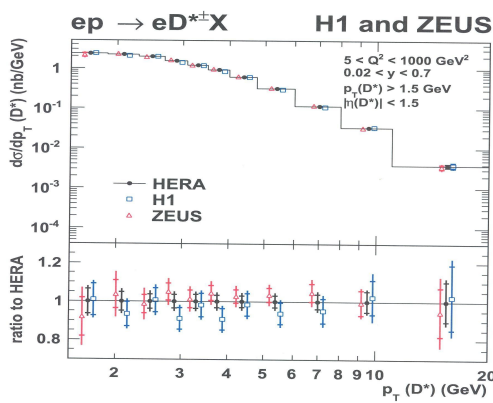
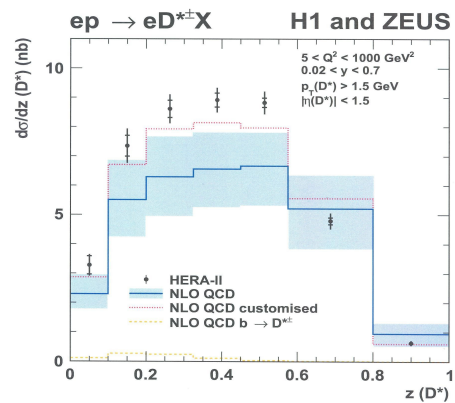


**Fig. 3:** Combined *H1* (blue) and *ZEUS* (red)  $d\sigma/dp_T(D^{*\pm})$  measured data - Fig. left.

**Fig. 4:** Combined *H1* and *ZEUS*  $d\sigma/dp_T(D^{*\pm})$  measured data compared to NLO QCD predictions. NLO QCD customized (red points.....) - Fig. right.

**Fig.5:** Combined *H1* and *ZEUS*  $d\sigma/dz(D^{*\pm})$  measured data compared to NLO QCD predictions. NLO QCD customized (red points.....).



Comparisons of the recorded data with the NLO QCD - HVQDIS predictions, seen in **Fig. 4**. and **Fig. 5**. (where the inner error bars indicate the uncorrelated part of the uncertainties, the outer error bars the total uncertainties and the bottom part in Fig. 4 shows the ratio of the cross sections with respect to the central value of the combined cross sections.), fits similarly rather well. Nevertheless, NLO QCD customization fits there still better.

Precision reached for the data  $\sim 5\%$  is good, but for the theory the precision reached is only  $\sim 30\%$  at low  $Q^2$ . It increases up to  $10\%$  for high  $Q^2$  values.

NLO QCD customization means to make precise study of the theory uncertainties. One try to vary the parameters used, e.g. pole mass of the **charm** quark to  $m_c = 1.35$  GeV, or to reduce or increase  $\mu_r$  and  $\mu_f$  scale by a factor 2, etc. Such a method describes often the data very well (see Fig. 7.). One can say, it shows a new possible way-direction for the future theory extension. One hopes that NNLO QCD calculations and several improved fragmentation models may also help in future to the next experimental data analyses. Similar conclusions are valid also for the double-differential cross section  $d^2\sigma/dQ^2dy(D^{*\pm})$  combinations seen in Figs. 6. and 7, (where the inner error bars indicate the uncorrelated part of the uncertainties, the outer error bars the total uncertainties).

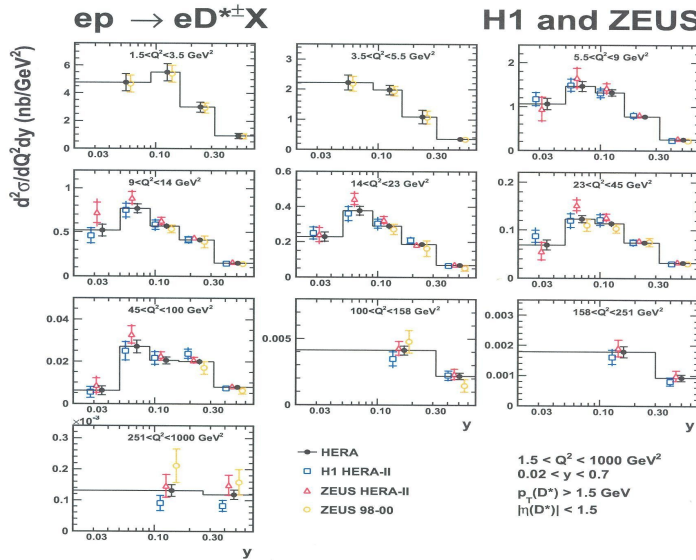


Fig. 6: *H1* and *ZEUS*  $d^2\sigma/dQ^2dy(D^{*\pm})$  measured data and the common combinations.

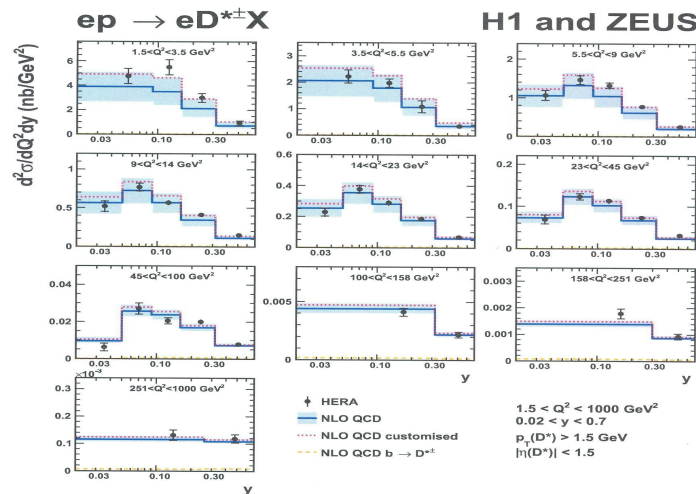


Fig. 7: Combined *H1* and *ZEUS*  $d^2\sigma/dQ^2dy(D^{*\pm})$  measured data compared to NLO QCD predictions. NLO QCD customized (red points ...).

## 6. Summary

$D^{*\pm}$  - production cross-section data in  $e-p$  DIS in *H1* and *ZEUS* experiments are combined at the level of visible cross-sections, accounting for their systematic correlations.

- \* data sets were consistent and the combination reduced significantly their uncertainties.
- \* combination has no significant theory-related uncertainties.
- \* several kinematic variables of  $D^{*\pm}$  are presented.
- \* combined data are compared to NLO QCD.
- \* NLO predictions describe the data rather well within their uncertainties.
- \* Higher order calculations could help to reduce theory uncertainties nearer to experimental data precision.
- \* Further improvements in heavy-quark fragmentation treatment are desirable.

## References

- [1] H. Abramowicz *et al.* [H1 and ZEUS Collaborations], *Combination of differential  $D^{*\pm}$  cross-section measurements in deep-inelastic ep scattering at HERA*, *JHEP09* (2015) 149 [arXiv:1503.06042].
- [2] E. Laenen *et al.* *Nucl.Phys.* **B392**, (1993) 229,  
S. Riemersma *et al.* *Phys. Lett.* **B347**, (1995) 143 [hep-ph/9411431].
- [3] B. W. Harris and J. Smith, *Phys. Rev.* **D57**, (1998) 2806 [hep-ph/9706334]
- [4] HERAFitter-0.2.1, [<http://projects.hepforge.org/herafitter>].